

# MUSIC and Aromatic Residues: Amino Acid Type-Selective $^1\text{H}$ – $^{15}\text{N}$ Correlations, III

Mario Schubert,<sup>\*,†</sup> Hartmut Oschkinat,<sup>\*,†</sup> and Peter Schmieder<sup>\*,1</sup>

<sup>\*</sup>Forschungsinstitut für Molekulare Pharmakologie, Robert-Rössle-Str. 10, D-13125 Berlin, Germany; and <sup>†</sup>Fachbereich Chemie, Pharmazie und Biologie, Freie Universität Berlin, Takustrasse 3, 14195 Berlin, Germany

Received April 30, 2001; revised August 23, 2001; published online November 7, 2001

Amino acid type-selective experiments can help to remove ambiguities in automated assignment procedures for  $^{15}\text{N}/^{13}\text{C}$ -labeled proteins. Here we present five triple-resonance experiments that yield amino acid type-selective  $^1\text{H}$ – $^{15}\text{N}$  correlations for aromatic amino acids. Four of the novel experiments are based on the MUSIC coherence transfer scheme that replaces the initial INEPT transfer and is selective for  $\text{CH}_2$ . The MUSIC sequence is combined with selective excitation pulses to create experiments for Trp (W-HSQC) as well as Phe, Tyr, and His (FYH-HSQC). In addition, an experiment selective for Trp  $\text{H}^{\epsilon 1}$ – $\text{N}^{\epsilon 1}$  is presented. The new experiments are recorded as two-dimensional experiments and their performance is demonstrated with the application to a protein domain of 115 amino acids. © 2001 Elsevier Science

**Key Words:** amino acid type-selective experiments; triple resonance; proteins; editing; HSQC; assignment.

## INTRODUCTION

For protein structure determination by NMR an almost complete sequential assignment of the  $^1\text{H}$ ,  $^{13}\text{C}$ , and  $^{15}\text{N}$  signals is crucial (1, 2). Today, 3D and 4D triple-resonance experiments (3, 4) and  $^{15}\text{N}/^{13}\text{C}$ -labeled proteins (5) are used routinely for the assignment procedure (6). The frequencies of the amide protons and the nitrogens are recorded in most of these techniques; therefore most assignment protocols use a  $^{15}\text{N}$  HSQC spectrum as a starting point and correlate the ( $^1\text{H}$ ,  $^{15}\text{N}$ ) frequency pairs with carbon or proton frequencies to achieve a sequence specific assignment.

We have recently presented several amino acid type-selective  $^1\text{H}$ ,  $^{15}\text{N}$  correlations (7, 8) that were designed to support this assignment strategy, in particular if an automated assignment protocol is used. Since the new experiments provide information on the type of amino acid, they will help to map the sequence of spin systems extracted from the spectra onto the amino acid sequence. The experiments are based on the MUSIC (multiplicity selective *in*-phase coherence transfer) pulse sequence building block (9), which accomplishes a coherence transfer to or from

the heteronucleus, selective for either  $\text{XH}_2$  or  $\text{XH}_3$  (where  $X$  can be  $^{15}\text{N}$  or  $^{13}\text{C}$ ) and has been derived from the POMMIE sequence (10, 11). By implementing MUSIC in triple-resonance experiments a selection of the topology of the amino acid side chain is possible.

Here, an extension of this set of selective  $^1\text{H}$ – $^{15}\text{N}$  correlations by another five experiments is presented. Two are based on the selection of Phe, Tyr, and His (FYH-HSQC), and two on the selection of Trp (W-HSQC). A pair of experiments that contain all four aromatic amino acids is also feasible. For each selection we designed two experiments: either signals from the sequential neighbors of the selected residue appear in the spectra ( $i + 1$  version) or signals of the selected residues themselves appear together with smaller signals from sequential neighbors ( $i$ ,  $i + 1$  version). The latter experiments are somewhat less sensitive. To accomplish the desired selection, the MUSIC step is combined with the use of selective pulses. Thus the chemical shifts of the side chain carbon atoms are used as additional criteria for the selection of an amino acid. In the resulting spectra the clean selection of the MUSIC step is enhanced by selective pulses, which make use of the distinct  $^{13}\text{C}$  chemical shifts of aromatic carbons. Additionally, a correlation selective for the  $\text{H}^{\epsilon 1}$ – $\text{N}^{\epsilon 1}$  pair of tryptophanes which makes use solely of selective pulses is presented. All experiments are applied to the EVH1 domain from VASP (12, 13), a protein of 115 residues, for which nitrogen relaxation experiments yield a rotational correlation time of 7.7 ns. The HSQC is shown in Fig. 1.

## RESULTS

The new sequences are closely related to the DNG experiments presented recently (8). All are derived from the CBCA(CO)NH (14) and CBCANH (15) experiments by replacing the initial refocused INEPT by a MUSIC element that selects for  $\text{CH}_2$  groups. To select only the desired methylene carbons, the MUSIC element is combined with an HMQC-like sequence (16, 17) with shaped  $90^\circ$  pulses. While the chemical shifts of adjacent carbonyl carbons are exploited as an additional selection criterion in the DNG experiments, in the new experiments the chemical shifts of the adjacent aromatic  $\text{C}'$  carbons, are

<sup>1</sup> To whom correspondence should be addressed. E-mail: [schmieder@fmp-berlin.de](mailto:schmieder@fmp-berlin.de).

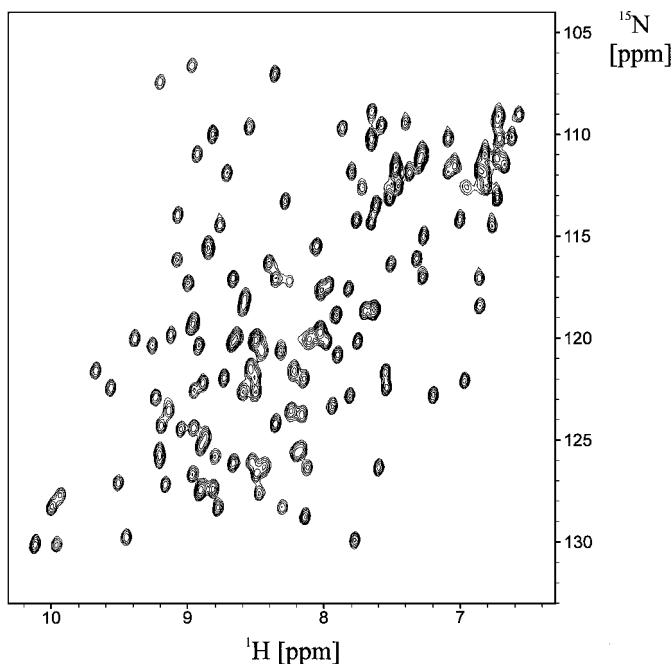


FIG. 1. The  $^{15}\text{N}$  HSQC of the EVH1 domain from VASP (12), a protein of 115 residues as a comparison for the spectra from the new selective experiments (Fig. 5).

used. During the HMQC-like sequence  $2C^{\beta}C^{\gamma}$  double-quantum coherence is selected by phase cycling. Subsequently, the magnetization is transferred from the  $C^{\beta}$  to the  $C^{\alpha}$ . From the  $C^{\alpha}$ , the magnetization is relayed either via the carbonyl carbon to the  $(i + 1)$  nitrogen or directly to both nitrogens coupled to the  $C^{\alpha}$  ( $i$  or  $i + 1$ ). The signal is finally detected on the respective amide protons. The transfer of magnetization is depicted schematically in Fig. 2, and the new pulse sequences in Figs. 3a and 3b.

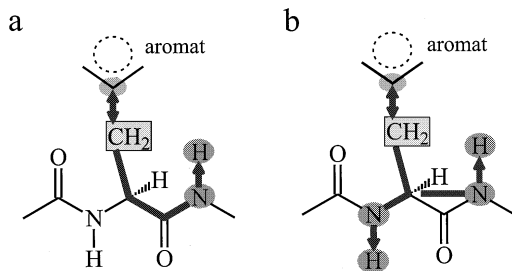


FIG. 2. Schematic representation of the magnetization pathway selected by the novel FYH and W experiments. First the  $\text{CH}_2$  group (indicated by a rectangle) is selected with the MUSIC sequence. In an out-and-back manner multiple quantum coherence including the aromatic  $C^{\gamma}$  nuclei is created and selected. From the  $C^{\beta}$ , the magnetization is transferred to the  $C^{\alpha}$  carbon and finally to the amide proton, as indicated by the arrows. The two types of pulse sequences differ in the transfer from the  $C^{\alpha}$  to the nitrogen. In the  $(i + 1)$ -HSQCs (left column), magnetization is transferred from the  $C^{\alpha}$  to the carbonyl and then to the nitrogen and amide proton. The right column represents the  $(i, i + 1)$ -HSQCs, where the magnetization is transferred from the  $C^{\alpha}$  to either the nitrogen of the same amino acid or that of the  $(i + 1)$  neighbor.

Self-refocusing LOS2-0 pulses (18, 19) which affect only aromatic  $C^{\gamma}$  carbons are used. This selection requires relatively long selective pulses. Since the  $J_{C^{\beta}C^{\alpha}}$  and  $J_{C^{\beta}C^{\gamma}}$  couplings are active during the selective pulse, the delay  $\Delta_1$  must be adjusted to compensate for this. The effective coupling between the  $C^{\beta}$  and  $C^{\gamma}$  carbon during the pulse is reduced and was determined experimentally to be 60% of the coupling during a free precession period. The resulting transfer functions for the selected amino acids in the experiments in Figs. 3a and 3b are therefore

$$\sin^2(\pi J_{C^{\beta}C^{\gamma}}(\Delta_1 + 0.6P)) \sin(\pi J_{C^{\alpha}C^{\beta}}(2\Delta_1 + 2P)) \times \sin(\pi J_{C^{\alpha}C^{\beta}}2\Delta_2) \sin(\pi J_{C^{\alpha}C^{\gamma}}2\Delta_2) \quad [1]$$

$$\sin^2(\pi J_{C^{\beta}C^{\gamma}}(\Delta_1 + 0.6P)) \sin(\pi J_{C^{\alpha}C^{\beta}}(2\Delta_1 + 2P)) \times \sin(\pi J_{C^{\alpha}C^{\beta}}2\Delta_3) \sin(\pi J_{C^{\alpha}N}2\Delta_3), \quad [2]$$

where  $P$  is the pulse length of the LOS2-0 pulses. Note that the value for the  $J_{C^{\beta}C^{\gamma}}$  coupling constants depends on the type of aromatic amino acid (20).

The  $^{13}\text{C}$  chemical shift ranges of the  $C^{\gamma}$  of Tyr, Phe, His, and Trp are shown in Fig. 4 (21). A self-refocusing LOS2-0 pulse with a duration of  $640 \mu\text{s}$  centered at 120 ppm covers the full range of all aromatic  $C^{\gamma}$  carbons. A more detailed view shows that the area of the  $^{13}\text{C}$  chemical shift of the  $C^{\gamma}$  of Tyr, Phe, and His is well separated from the  $C^{\gamma}$  of Trp. Therefore, selective pulses with a narrower bandwidth were chosen to select Phe, Tyr, and His or Trp.

### Selecting His, Phe, Tyr: The FYH- $(i + 1)$ - and FYH- $(i, i + 1)$ -HSQC

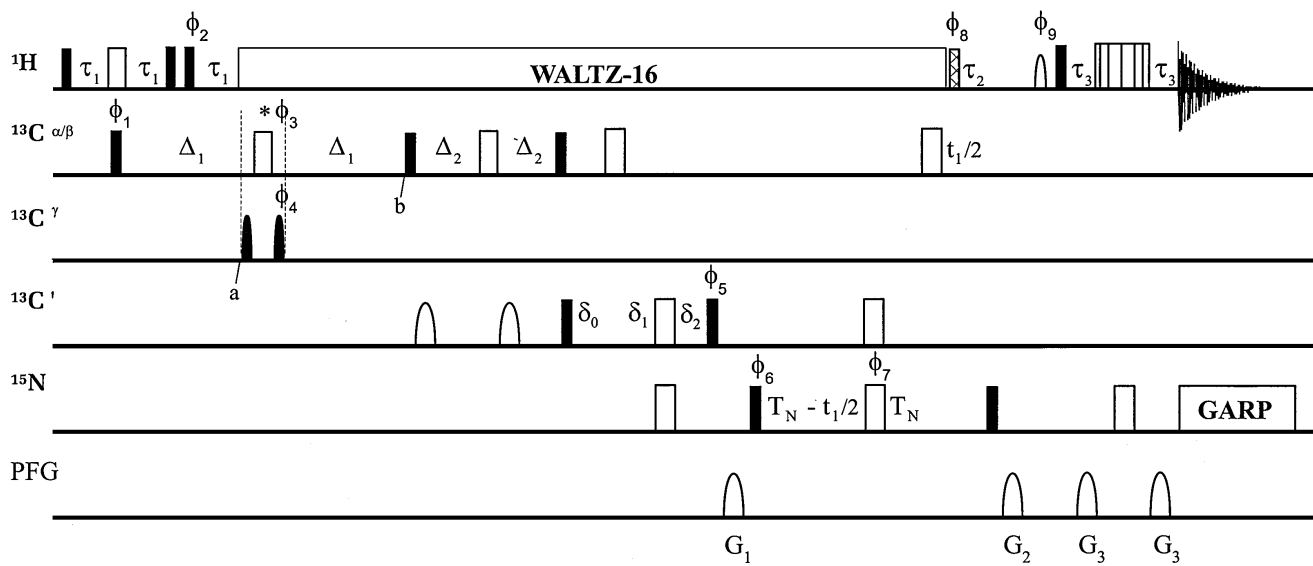
To excite and select only the  $C^{\gamma}$  of His, Phe, and Tyr but not of Trp, a selective pulse covering a range of 5000 Hz (33 ppm at 600 MHz) centered at 135 ppm is necessary. Self-refocusing LOS2-0 pulses (18, 19) with a duration of  $1024 \mu\text{s}$  were applied. The rectangular  $180^\circ$  pulse in between the LOS2-0 pulses was executed at 45 ppm and was adjusted to have a null in the excitation profile at 125 ppm. Assuming a  $J_{C^{\beta}C^{\gamma}} = 44 \text{ Hz}$  (20) and neglecting relaxation effects, nominal values for  $\Delta_1$ ,  $\Delta_2$ , and  $\Delta_3$  are 8.15, 5.3, and 9 ms, respectively. However, after experimental optimization, values for  $\Delta_1$ ,  $\Delta_2$ , and  $\Delta_3$  were chosen to be 6.7, 4.5, and 9 ms, respectively.

The resulting spectra will only contain signals originating from His, Phe, and Tyr and are shown in Figs. 5a and 5b.

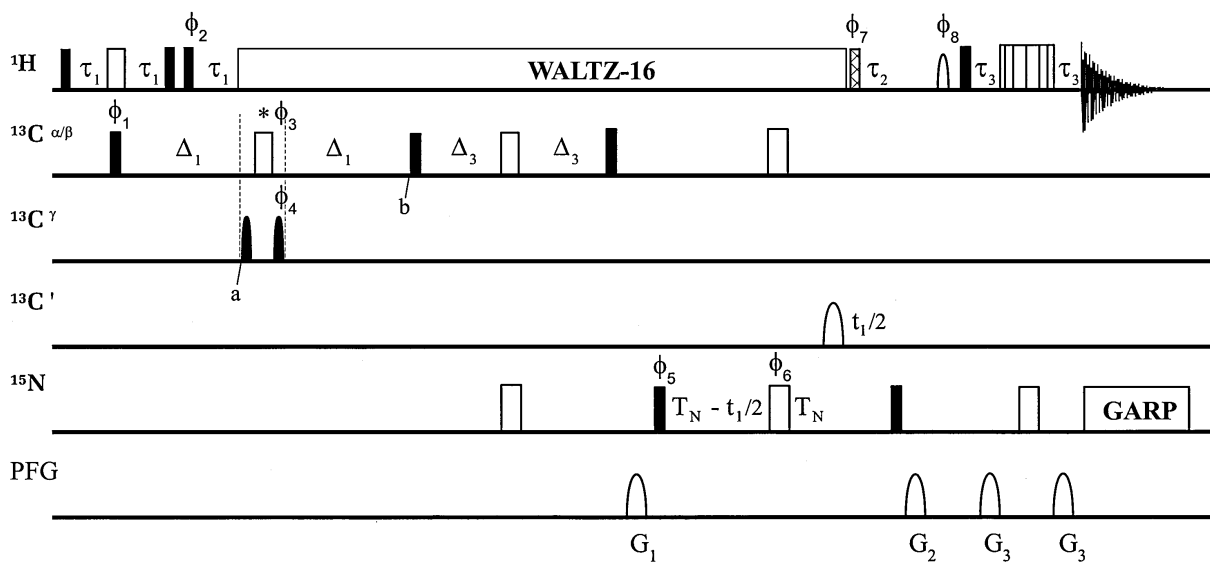
### Selecting Trp: The W- $(i + 1)$ - and W- $(i, i + 1)$ -HSQC

To select Trp residues but not Tyr, His, and Phe, the same LOS2-0 pulses as in the FYH experiments but centered at 105 ppm were used (Fig. 4). The offset of the rectangular  $180^\circ$  pulse in between the LOS2-0 pulses is now set to 30 ppm and adjusted to exhibit a null in the excitation profile at 110 ppm.

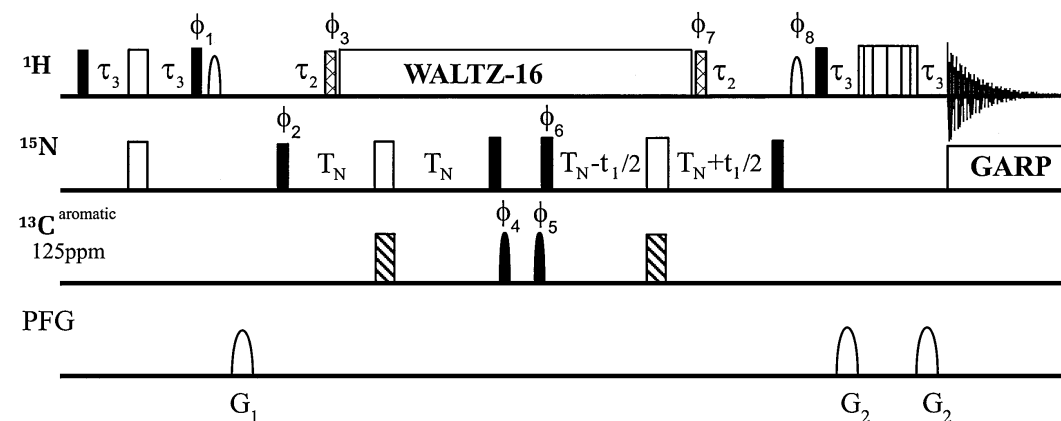
a



b



c



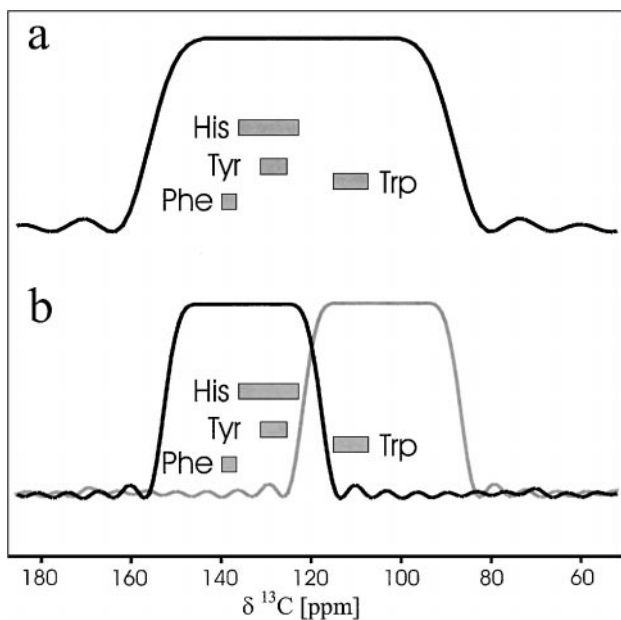


**FIG. 4.** The  $^{13}\text{C}$  chemical shift distribution for the  $\text{C}^\gamma$  of the aromatic amino acids taken from the BioMagRes database (21) and the excitation profiles of the LOS2-0 pulses: (a) with a length of  $640\ \mu\text{s}$  to select all aromatic amino acids at 120 ppm and (b) with a length of  $1024\ \mu\text{s}$  at either 135 or 105 ppm to select Phe, Tyr, and His or solely Trp.

Using a  $J_{\text{C}^\beta\text{C}^\gamma} = 46.6\ \text{Hz}$  (20) and neglecting relaxation effects, the nominal value for  $\Delta_1$  is 7.95 ms. The best signal-to-noise ratio was found with a value of 6.5 ms for  $\Delta_1$ . The values for the delays  $\Delta_2$  and  $\Delta_3$  are identical to those for the FYH experiments. The resulting spectra contain only signals originating from Trp and are shown in Figs. 5c and 5d.

For the suppression of signals from amino acids other than the desired ones, calibration of the two selective  $90^\circ$  pulses turned out to be critical. If these pulses are not calibrated properly, resonances outside the ranges shown in Fig. 4 are excited as well and breakthrough peaks appear in the spectra. Signals from Asn/Asp and Ser show up most easily.

### Selecting Trp $\text{H}^{\epsilon 1}\text{N}^{\epsilon 1}$ : The $\text{H}^{\epsilon 1}\text{N}^{\epsilon 1}$ HSQC

As an aid for the further assignment of the  $^1\text{H}$ - $^{15}\text{N}$  correlations, an experiment for the indole NH of Trp was created. This experiment correlates the  $^1\text{H}$  and  $^{15}\text{N}$  chemical shifts of the  $\text{H}^{\epsilon 1}\text{N}^{\epsilon 1}$  group. It makes use of the distinct chemical shift of the aromatic carbons  $\text{C}^{\delta 1}$  and  $\text{C}^{\epsilon 2}$  adjacent to the indole nitrogen. The pulse sequence is a 2D version of an HNCA-like experiment; however, the  $^{13}\text{C}$  offset is changed to 125 ppm (Fig. 3c). The selectivity is achieved by using LOS2-0 pulses (18, 19) with a length of  $512\ \mu\text{s}$  as  $90^\circ$  pulses and REBURP pulses (22) with a length of  $1024\ \mu\text{s}$  as  $180^\circ$  pulses on the carbon channel. The

**FIG. 3.** Pulse sequences of the new amino acid type-selective  $^1\text{H}$ - $^{15}\text{N}$  correlations. The pulse sequences yield spectra selective for His/Phe/Tyr or solely Trp, depending on the choice of the offset for the LOS2-0 pulses. The pulse sequence for the  $(i+1)$ -HSQCs is shown in (a) that for the  $(i, i+1)$ -HSQCs in (b), the sequence for the Trp selective  $\text{H}^{\epsilon 1}\text{N}^{\epsilon 1}$  correlation in (c). Narrow filled and wide unfilled rectangles correspond to  $90^\circ$  and  $180^\circ$  rectangular pulses, respectively. Water-selective  $90^\circ$   $^1\text{H}$  flip-back pulses are represented by sine shapes; a hatched thin bar stands for a  $90^\circ$  flip-back  $^1\text{H}$  pulse at the end of the  $^1\text{H}$ -decoupling sequence. Magnetic field gradients as well as shaped  $180^\circ$   $^{13}\text{CO}$  pulses are represented by sine shapes. Pulses applied at the  $^{13}\text{C}^{\alpha/\beta}$  or  $^{13}\text{CO}$  resonance frequencies were adjusted to provide a null at the corresponding  $^{13}\text{CO}$  or  $^{13}\text{C}^\alpha$  frequencies. The rectangular  $^{13}\text{C}^{\alpha/\beta}$   $90^\circ$  and  $180^\circ$  pulses were set to 49 and 44  $\mu\text{s}$ , respectively. The rectangular  $^{13}\text{CO}$   $90^\circ$  and  $180^\circ$  pulses were set to 54 and 108  $\mu\text{s}$ , respectively. The rectangular  $^{13}\text{C}^{\alpha/\beta}$   $180^\circ$  pulses with an asterisk were set to 72  $\mu\text{s}$  and provide a null at the corresponding  $^{13}\text{C}^\gamma$  frequencies. The shaped  $180^\circ$   $^{13}\text{CO}$  were applied as G3 Gaussian cascade (26) with a duration of 256  $\mu\text{s}$ . The striped thick bars stand for band-selective  $180^\circ$  REBURP pulses (22). The offsets and pulse lengths are given in the description of the particular experiments. Self-refocusing selective LOS2-0 excitation pulses (18, 19) are represented by filled sine shapes. The second LOS2-0 pulse has a time inverted shape. The pulse lengths are given in the section of the particular experiment. Unless indicated otherwise, pulses are applied with phase  $x$ . Proton hard pulses were applied with 25-kHz field strength; WALTZ-16 decoupling (27) of  $^1\text{H}$  spins was achieved using a field strength of 3.1 kHz. The same field strength was used for the subsequent  $90^\circ$  flip back  $^1\text{H}$  pulse. The water-selective  $90^\circ$  rectangular pulse had a duration of 1 ms. GARP-1 decoupling (28) of  $^{15}\text{N}$  was achieved using a field strength of 830 Hz. Water suppression was obtained using WATERGATE implemented with a 3–9–19 pulse (29). The gradients were applied as a sinusoidal function from 0 to  $\pi$ . The carrier frequencies were centered at  $^1\text{H} = 4.8\ \text{ppm}$ ,  $^{15}\text{N} = 119.6\ \text{ppm}$ ,  $^{13}\text{C}^\alpha = 55\ \text{ppm}$ ,  $^{13}\text{C}^{\alpha/\beta} = 45\ \text{ppm}$ ,  $^{13}\text{C}^\gamma = 135\ \text{ppm}$  for FYH and 105 ppm for W (see text), and  $^{13}\text{CO} = 175\ \text{ppm}$ . The following delays were used:  $\tau_1 = 3.5\ \text{ms}$ ,  $\tau_2 = 5.5\ \text{ms}$ ,  $\tau_3 = 2.25\ \text{ms}$ ,  $\delta_0 = 4.5\ \text{ms}$ ,  $\delta_1 = 6.9\ \text{ms}$ ,  $\delta_2 = 11.4\ \text{ms}$ ,  $T_N = 11\ \text{ms}$ ,  $T_R = 4\ \text{ms}$ ,  $\Delta_1 = 6.7\ \text{ms}$  for FYH and 6.5 ms for W,  $\Delta_2 = 4.5\ \text{ms}$ , and  $\Delta_3 = 9\ \text{ms}$ . To achieve quadrature detection in the indirect dimension the States–TPPI–States protocol (30) was used in all experiments. All spectra were processed using XWINNMR (Bruker AG). (a) FYH- $(i+1)$ -HSQC and W- $(i+1)$ -HSQC. The phase cycling was  $\phi_1 = 16(x), 16(-x); \phi_2 = 2(45^\circ), 2(135^\circ), 2(225^\circ), 2(315^\circ); \phi_3 = 32(x), 32(-x); \phi_4 = x, -x; \phi_5 = 50^\circ; \phi_6 = x; \phi_7 = 8(x), 8(y), 8(-x), 8(-y); \phi_8 = 4(-y), 4(y); \phi_9 = -x; \phi_{\text{rec}} = 2(x, 2(-x), x), 4(-x, 2(x), -x), 2(x, 2(-x), x)$ . States–TPPI phase cycling was applied to phase  $\phi_6$ . The LOS2-0 pulses had a duration of 1024  $\mu\text{s}$  and were applied at 135 ppm (FYH), 105 ppm (W), respectively. The rectangular  $180^\circ$  pulse marked with an asterisk was applied at 45 ppm in the FYH- $(i+1)$ -HSQC and at 30 ppm in the W- $(i+1)$ -HSQC. The gradients had the following duration and strength:  $G_1 = 1\ \text{ms}$  (7 G/cm),  $G_2 = 800\ \mu\text{s}$  (28 G/cm),  $G_3 = 1\ \text{ms}$  (21 G/cm). (b) FYH- $(i, i+1)$ -HSQC and W- $(i, i+1)$ -HSQC. The phase cycling was  $\phi_1 = 16(x), 16(-x); \phi_2 = 2(45^\circ), 2(135^\circ), 2(225^\circ), 2(315^\circ); \phi_3 = 32(x), 32(-x); \phi_4 = x, -x; \phi_5 = 64(x), 64(-x); \phi_6 = 8(x), 8(y), 8(-x), 8(-y); \phi_7 = 4(-y), 4(y); \phi_8 = -x; \phi_{\text{rec}} = 2(x, 2(-x), x), 4(-x, 2(x), -x), 4(x, 2(-x), x), 4(-x, 2(x), -x), 2(-x, 2(x), -x), 4(x, 2(-x), x), 4(-x, 2(x), -x), 4(x, 2(-x), x), 2(-x, 2(x), -x)$ . States–TPPI phase cycling was applied to phase  $\phi_5$ . The same selective pulses as in the FYW- $(i+1)$  and W- $(i+1)$  experiment were used. The gradients had the following duration and strength:  $G_1 = 1\ \text{ms}$  (7 G/cm),  $G_2 = 800\ \mu\text{s}$  (28 G/cm),  $G_3 = 1\ \text{ms}$  (21 G/cm). (c) Trp  $\text{H}^{\epsilon 1}\text{N}^{\epsilon 1}$  HSQC correlation. The phase cycling was  $\phi_1 = y; \phi_2 = 8(x), 8(-x); \phi_3 = y; \phi_4 = x, -x; \phi_5 = 4(x), 4(-x); \phi_6 = 2(x), 2(-x); \phi_7 = -y; \phi_8 = -x; \phi_{\text{rec}} = x, 2(-x), x, 2(-x, 2(x), -x), x, 2(-x), x$ . States–TPPI phase cycling was applied to phase  $\phi_6$ . The carrier frequency for  $^{13}\text{C}$  was centered at 125 ppm;  $180^\circ$  REBURP pulses with a duration of 1024  $\mu\text{s}$  and  $90^\circ$  LOS2-0 pulses with a duration of 512  $\mu\text{s}$  were used. The gradients had the following duration and strength:  $G_1 = 800\ \mu\text{s}$  (28 G/cm),  $G_2 = 1\ \text{ms}$  (21 G/cm).

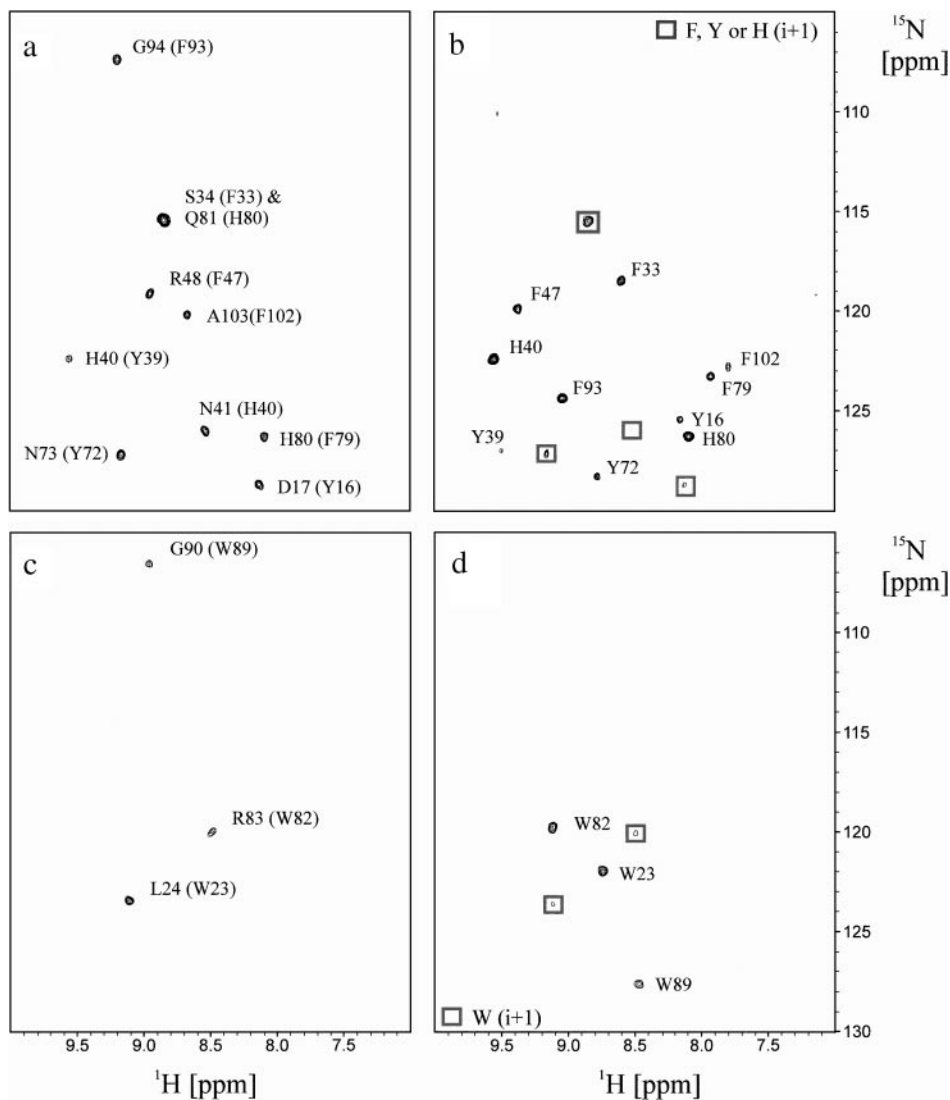


**FIG. 5.** Amino acid type-selective  $^1\text{H}$ - $^{15}\text{N}$  correlations of the EVH1 domain from VASP. The EVH1 domain contains 5 Phe, 3 Tyr, 2 His, and 3 Trp. (a) FYH- $(i+1)$ -HSQC, all expected signals are present. (b) FYH- $(i, i+1)$ -HSQC, signals from all His, Phe, and Tyr residues occur and of most of their sequential neighbors (marked with rectangles). (c) W- $(i+1)$ -HSQC, all three expected signals are visible. (d) W- $(i, i+1)$ -HSQC, the signals of all three Trp residues and two of their sequential neighbors (marked with rectangles) are present.

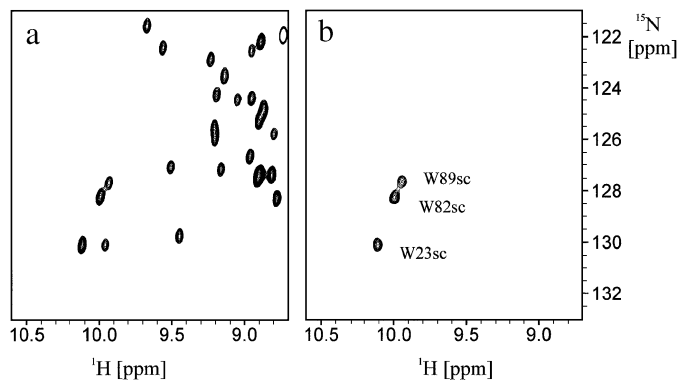


**FIG. 6.** Trp  $\text{H}^{\epsilon 1}\text{N}^{\epsilon 1}$  HSQC in comparison to a normal  $^{15}\text{N}$  HSQC of the EVH1 domain from VASP. (a) Region from the  $^{15}\text{N}$  HSQC shown in Fig. 1. (b) Trp  $\text{H}^{\epsilon 1}\text{N}^{\epsilon 1}$  HSQC, the three expected signals are present.

experiment is quite sensitive and can be recorded in a very short time; a comparison between the conventional HSQC and the  $\text{H}^{\epsilon 1}\text{N}^{\epsilon 1}$  HSQC is shown in Fig. 6.

## CONCLUSION

A new set of amino acid type-selective  $^1\text{H}$ - $^{15}\text{N}$  correlations has been presented. The FYH- $(i+1)$ - and W- $(i+1)$ -HSQC experiments select signals of sequential neighbors of His, Phe, and Tyr residues and of Trp residues, respectively, while the FYH- $(i, i+1)$ - and W- $(i, i+1)$ -HSQC experiments select signals from the residues themselves and of the sequential neighbors. The sequences are less sensitive than standard triple-resonance experiments because of the longer delays in the sequence and since less protons contribute to the overall signal.

A comparison of the signal-to-noise ratio of the new experiments and an  $^1\text{H}$ - $^{15}\text{N}$  version of the CBCA(CO)NNH yields a ratio of 1 : 8.

The new sequences will work well with medium size proteins up to 15 kDa. Since they cannot be applied to deuterated proteins, their application will be problematic with larger proteins and they will fail when the standard triple-resonance experiments usually applied to protonated proteins fail as well.

Together with the recently published selective  $^1\text{H}$ - $^{15}\text{N}$  correlations we now have a set of 24 experiments which allow us to identify the  $^1\text{H}$ - $^{15}\text{N}$  resonances of Gly, Ala, Thr, Ile/Val, Asn, Gln, Ser, Leu, Asp, Glu, His/Phe/Tyr, and Trp residues and their sequential neighbors in a  $^{15}\text{N}$  HSQC spectrum. In addition, we are able to identify amide signals of the preceding as well as succeeding residues of prolines (23) and  $^1\text{H}$ - $^{15}\text{N}$  resonances of the of tryptophan side chains.

This set of two-dimensional spectra can be used in addition to the conventional multidimensional spectra in an automated assignment procedure. The spectra require a small amount of spectrometer time compared to three-dimensional experiments and provide unambiguous information about the amino acid type, which is essential for a fast, automated sequence specific assignment. Conventionally, a probability for the type of the amino acid is obtained from the  $C^\alpha/C^\beta$  pair of chemical shifts but this procedure does normally not yield a single amino acid type. As an example we obtained the probabilities for the amino acid types of the three Trp residues in the EVH1 domain from their  $C^\alpha$  and  $C^\beta$  chemical shifts using the program type prob (24). The resulting probabilities for Trp are 20.7, 15.6, and 11.5% for W23, W82, and W89, respectively. There are 4, 2, and 5 other amino acids with probabilities higher than 10% for these three residues, respectively. This complicates a sequence specific assignment and it will be helpful to determine the amino acid type directly using the new amino acid selective experiments.

## EXPERIMENTAL

The spectra were recorded on a Bruker DRX600 in standard configuration using an inverse triple-resonance probe equipped with three-axis self-shielded gradient coils. The experiments were recorded with a 1.35 mM sample of the EVH1 domain from VASP uniformly labeled with  $^{15}\text{N}$  and  $^{13}\text{C}$ , and 5-mm ultra-precision sample tubes were used. All spectra were recorded in an identical way with  $64 (t_1) \times 512 (t_2)$  complex points and spectral widths of 3012 Hz ( $^{15}\text{N}$ )  $\times$  10,000 Hz ( $^1\text{H}$ ). The  $^{15}\text{N}$  HSQC was acquired in 12 min using 4 scans. The FYH-( $i + 1$ )-HSQC and the FYH-( $i, i + 1$ )-HSQC were acquired in 3 and 6 h using 64 and 128 scans, respectively. The same is true for the two Trp experiments. The  $\text{H}^{\epsilon 1}\text{N}^{\epsilon 1}$  HSQC was acquired in 24 min using 8 scans. The data were processed using a squared sinebell shifted by  $90^\circ$  as a window function in both dimensions. The  $^{15}\text{N}$   $t_1$  interferograms were quadrupled in length by linear prediction using XWINNMR. The resulting spectra had a size of  $512 (t_1) \times 1024 (t_2)$  real points and were analyzed using the program Sparky (25). The pulse programs and the L0S2-

0 shape in Bruker format are available under <http://www.fmp-berlin.de/~schubert>.

## ACKNOWLEDGMENTS

Support from the Forschungsinstitut für Molekulare Pharmakologie is gratefully acknowledged. Mario Schubert is supported by the DFG Graduiertenkolleg GRK 80 "Modellstudien." The authors thank Frank Löhner, Rüdiger Winter, Dietmar Leitner, Dirk Labudde, and Wolfgang Bermeil for helpful discussions, Linda Ball for the assignment of the EVH1 domain, Thomas Jarchau for the preparation of the EVH1 sample, and Grant Langdon for carefully reading the manuscript. The work was supported by a grant of the BMBF (01 GG 9812, Leitprojekt "Proteinstrukturfabrik").

## REFERENCES

1. K. Wüthrich, "NMR of Proteins and Nucleic Acids," Wiley, New York (1986).
2. J. Cavanagh, W. J. Fairbrother, A. G. Palmer III, and N. J. Skelton, "Protein NMR Spectroscopy," Academic Press, San Diego (1996).
3. G. T. Montelione and G. Wagner, Conformation-independent sequential NMR connections in isotope-enriched polypeptides by  $^1\text{H}$ - $^{13}\text{C}$ - $^{15}\text{N}$  triple-resonance experiments, *J. Magn. Reson.* **87**, 183–188 (1990).
4. L. E. Kay, M. Ikura, R. Tschudin, and A. Bax, Three-dimensional triple-resonance NMR spectroscopy of isotopically enriched proteins, *J. Magn. Reson.* **89**, 496–514 (1990).
5. L. P. McIntosh and F. W. Dahlquist, Biosynthetic incorporation of  $^{15}\text{N}$  and  $^{13}\text{C}$  for assignment and interpretation of nuclear magnetic resonance spectra of proteins, *Quart. Rev. Biophys.* **23**, 1 (1990).
6. G. M. Clore and A. M. Gronenborn, Application of three- and four-dimensional heteronuclear NMR spectroscopy to protein structure determination, *Prog. NMR Spectrosc.* **23**, 43–92 (1991).
7. M. Schubert, M. Smalla, P. Schmieder, and H. Oschkinat, MUSIC in triple-resonance experiments: Amino acid type-selective  $^1\text{H}$ - $^{15}\text{N}$  correlations, *J. Magn. Reson.* **141**, 34–43 (1999).
8. M. Schubert, H. Oschkinat, and P. Schmieder, MUSIC, selective pulses and tuned delays: Amino acid type-selective  $^1\text{H}$ - $^{15}\text{N}$  correlations, II, *J. Magn. Reson.* **148**, 61–72 (2001).
9. P. Schmieder, M. Leidert, M. Kelly, and H. Oschkinat, Multiplicity-selective coherence transfer steps for the design of amino acid-selective experiments—A triple-resonance experiment selective for Asn and Gln, *J. Magn. Reson.* **131**, 199–202 (1998).
10. M. H. Levitt and R. R. Ernst, Multiple-quantum excitation and spin topology filtration in high-resolution NMR, *J. Chem. Phys.* **83**, 3297–3310 (1983).
11. J. M. Bulsing, W. M. Brooks, J. Field, and D. M. Doddrell, Polarization transfer via an intermediate multiple-quantum state of maximum order, *J. Magn. Reson.* **56**, 167–173 (1984).
12. L. J. Ball, R. Kuhne, B. Hoffmann, A. Hafner, P. Schmieder, R. Volkmer-Engert, M. Hof, M. Wahl, J. Schneider-Mergener, U. Walter, H. Oschkinat, and T. Jarchau, Dual epitope recognition by the VASP EVH1 domain modulates polyproline ligand specificity and binding affinity, *EMBO J.* **19**, 4903–4914 (2000).
13. I. Callabaut, P. Crossart, and P. Dehoux, EVH1/WH1 domains of VASP and WASP proteins belong to a large family including Ran-binding domains of RanBP1 family, *FEBS Lett.* **441**, 181–185 (1999).
14. S. Grzesiek and A. Bax, Correlating backbone amide and side chain resonances in larger proteins by multiple relayed triple resonance NMR, *J. Am. Chem. Soc.* **114**, 6291–6293 (1992).
15. S. Grzesiek and A. Bax, An efficient experiment for sequential backbone assignment of medium-sized isotopically enriched proteins, *J. Magn. Reson. B* **99**, 201–207 (1992).

16. L. Müller, Sensitivity enhanced detection of weak nuclei using heteronuclear multiple quantum coherence, *J. Am. Chem. Soc.* **101**, 4481–4484 (1979).
17. A. Bax, R. H. Griffey, and B. L. Hawkins, Correlation of proton and nitrogen-15 chemical shifts by multiple quantum NMR, *J. Magn. Reson.* **55**, 301–315 (1983).
18. E. Lunati, P. Cofrancesco, M. Villa, P. Marzola, and F. Osculati, Evolution strategy optimization for selective pulses in NMR, *J. Magn. Reson.* **134**, 223–235 (1998).
19. <http://matsci.unipv.it/persons/lunati/pulses.htm>.
20. F. Löhr, C. Pérez, R. Köhler, H. Rüterjans, and J. Schmidt, Heteronuclear relayed E.COSY revisited: Determination of  $^3J(\text{H}^\alpha\text{C}^\gamma)$  couplings in Asx and aromatic residues in proteins, *J. Biomol. NMR* **18**, 13–22 (2000).
21. <http://www.bmrwisc.edu/>.
22. H. Geen and R. Freeman, Band-selective radiofrequency pulses, *J. Magn. Reson.* **93**, 93–141 (1991).
23. M. Schubert, L. J. Ball, H. Oschkinat, and P. Schmieder, Bridging the gap: A set of selective  $^1\text{H}$ – $^{15}\text{N}$ -correlations to link sequential neighbors of prolines, *J. Biomol. NMR* **17**, 331–335 (2000).
24. S. Grzesiek and A. Bax, Amino acid type determination in the sequential assignment procedure of uniformly  $^{13}\text{C}/^{15}\text{N}$ -enriched proteins, *J. Biomol. NMR* **3**, 185–204 (1993).
25. T. D. Goddard and D. G. Kneller, SPARKY 3, University of California, San Francisco; <http://www.cgl.ucsf.edu/home/sparky/>.
26. L. Emsley and G. Bodenhausen, Gaussian pulse cascades: New analytical functions for rectangular selective inversion and in-phase excitation in NMR, *Chem. Phys. Lett.* **165**, 469–476 (1990).
27. A. J. Shaka, J. Keeler, T. Frenkiel, and R. Freeman, An improved sequence for broadband decoupling: WALTZ-16, *J. Magn. Reson.* **52**, 335–338 (1983).
28. A. J. Shaka, P. B. Barker, and R. Freeman, Computer-optimized decoupling scheme for wideband applications and low-level operation, *J. Magn. Reson.* **64**, 547–552 (1985).
29. V. Sklenar, M. Piotto, R. Leppik, and V. Saudek, Gradient-tailored water suppression for  $^1\text{H}$ – $^{15}\text{N}$  HSQC experiments optimized to retain full sensitivity, *J. Magn. Reson. A* **102**, 241–245 (1993).
30. D. Marion, M. Ikura, R. Tschudin, and A. Bax, Rapid recording of 2D NMR spectra without phase cycling, application to the study of hydrogen exchange, *J. Magn. Reson.* **85**, 393–399 (1989).